Applied Surface Science 344 (2015) 52–56

Contents lists available at ScienceDirect

Applied Surface Science

journal homepage: www.elsevier.com/locate/apsusc

Proton irradiation energy dependence of defect formation in graphene

Sanggeun Lee[a], Jungmok Seo[a], Juree Hong[a], Seul Hyun Park[b], Joo-Hee Lee[b], Byung-Wook Min[c], Taeyoon Lee[a,*]

[a] Nanobio Device Laboratory, School of Electrical and Electronic Engineering, Yonsei University, 50 Yonsei-ro, Seodaemun-Gu, Seoul 120-749, Republic of Korea
[b] Space Science Research Team, Aerospace Convergence Technology Research Laboratory, Korea Aerospace Research Institute, 169-87 Gwahak-ro, Yuseong-Gu, Daejeon 305-806, Republic of Korea
[c] Microwave Integrated Circuits and Systems Laboratory, School of Electrical and Electronic Engineering, Yonsei University, 50 Yonsei-ro, Seodaemun-Gu, Seoul 120-749, Republic of Korea

ARTICLE INFO

Article history:
Received 27 January 2014
Received in revised form 29 January 2015
Accepted 19 March 2015
Available online 25 March 2015

Keywords:
Graphene
Cosmic ray
Proton irradiation
Raman spectroscopy

ABSTRACT

Graphene transistors on SiO_2/Si were irradiated with 5, 10, and 15 MeV protons at a dose rate of 2×10^{14} cm^{-2}. The effect of proton irradiation on the structural defects and electrical characteristics of graphene was measured using Raman spectroscopy and electrical measurements. Raman spectra exhibited high intensity peaks induced by defects after 5 and 10 MeV proton irradiation, whereas no significant defect-induced peaks were observed after 15 MeV proton irradiation. The drain current of graphene transistors decreased and the Dirac point shifted after proton irradiation; however, a flattening in the Dirac point occurred after 15 MeV proton irradiation. The variations in characteristics were attributed to different types of graphene defects, which were closely related to the irradiation energy dependency of the transferred energy. Our observation results were in good agreement with the Bethe formula as well as the stopping and range of ions in matter simulation results.

Electronic devices used in outer space and low earth orbit suffer from radiation-induced atomic displacements generated by cosmic rays [1], which are composed of highly energetic particles of mostly protons originated from the supernova of massive stars [2]. Thus, high radiation hardness is crucial for the operation of such devices in aerospace conditions. In order to prevent such damages, a high threshold displacement energy (T_d) of the material is needed, which is the minimum kinetic energy required to displace an atom from its lattice. When highly energetic particles bombard a target, they can transfer enough energy to displace atoms and form defects. Therefore, T_d must be large to prevent displacements that can degrade the device performance. Experimental results show that T_d varies inversely to the lattice constant [3]. For example, GaN (a = 0.319 nm and c = 0.519 nm for hexagonal) is a better candidate for radiation hardness compared to other semiconductors such as Si (a = 0.543 nm) and GaAs (a = 0.5653 nm for zinc-blende) [4–6] which have a larger lattice constant. The probability of defect formation can also be reduced by using atomically thin electrical channels. When highly energetic protons are incident, they penetrate and create defects in the target. If the electrical channel is thin, then the probability of defect formation inside the electrical channel is much lower than the bulk. Specifically, by using few nanometer thick electrical channels such as two dimensional electron gas (2DEG) [7], the probability of a defect center forming inside the channel by irradiation is smaller compared to the bulk material [4,6].

In this respect, graphene can be considered as a promising candidate for aerospace applications. Graphene is one of the strongest materials that has ever been reported, with an intrinsic tensile strength of 130 GPa and a Young's modulus of 1 TPa [8]. It also has a small lattice constant of a = 0.246 nm, thus graphene can be expected to have a large T_d value. Theoretical and experimental T_d value of graphene is 18–22 eV [9], which is much larger than the nitrogen T_d of GaN [3]. In addition, as the one-atom thick graphene has a small thickness of 0.34 nm, the probability of defect formation in graphene from an incident proton will be very small. Despite these advantages, there are only a few experimental reports on graphene irradiated by highly energetic protons in the mega-electronvolt range [10–12], none of which have investigated the dependency of proton energy, which is essential for the study of degradation mechanisms [6].

In this paper, we report on the formation of defects in graphene on SiO_2/Si substrates irradiated with protons with energies of 5, 10 and 15 MeV at a fixed fluence of 2×10^{14} cm^{-2}. Using Raman

* Corresponding author. Tel.: +82 2 2123 5767; fax: +82 2 313 2879.
E-mail address: taeyoon.lee@yonsei.ac.kr (T. Lee).

http://dx.doi.org/10.1016/j.apsusc.2015.03.107
0169-4332/

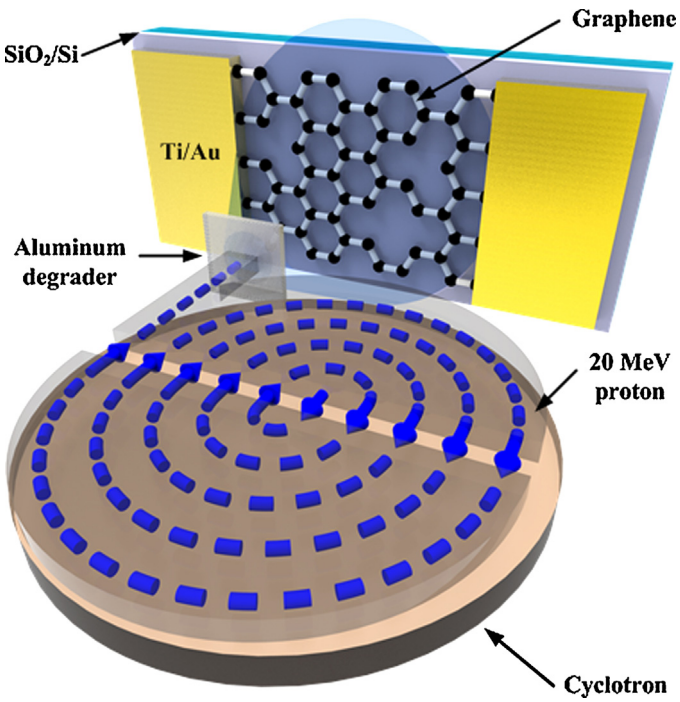

Fig. 1. Schematic of the experimental setup and device structure. Samples were placed inside the proton beam which was decelerated from a 20 MeV source to a target energy of 5, 10, and 15 MeV at a constant dose of 2×10^{14} cm^{-2}.

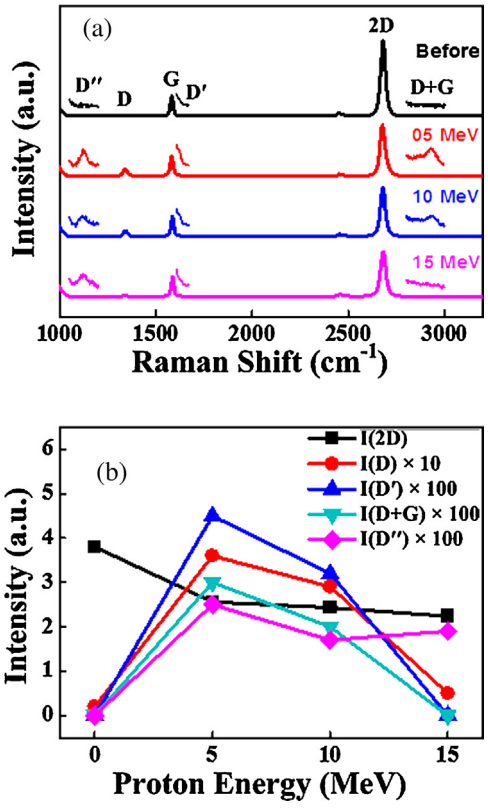

Fig. 2. (a) Raman spectrum of graphene before and after proton irradiation. The D″, D′, and D + G peaks are magnified by 30, 10, and 30 times respectively. (b) Peak intensities normalized to the G peak before irradiation.

spectroscopy and electrical measurements, we show that the characteristics of graphene differ depending on the irradiated proton energy. Specifically, protons with 5 and 10 MeV increased the D and D′ peaks which corresponding to vacancy related defects, while irradiation with 15 MeV did not cause a significant increase in such peaks. Instead, a slight increase of the D″ peak was observed for 15 MeV, which is normally observed for defective sp^3 carbons. The transfer curve showed as decrease in the current and shifts of the Dirac point after 5 and 10 MeV proton irradiation, while irradiation with 15 MeV resulted in flattening at the Dirac point. The inconsistency among these results was attributed to the different types of defects caused by irradiated energy dependency of the transferred energy from energetic protons. Further, theoretical and simulation results indicated that the differences were due to the lower energy transferred to graphene from higher energy protons.

Graphene was grown on 25-μm-thick copper foils (Alfa Aesar, #13382) using a conventional split tube furnace [13]. 200 sccm (standard cubic centimeters per minute) of H_2 gas was inserted while the temperature was elevated to 1000 °C over a period of 20 min. The Cu foil was annealed for another 20 min at the same conditions and then 40 sccm of CH_4 was inserted for 30 min followed by natural cooling to room temperature. PMMA (average molecular weight ~996,000, Sigma–Aldrich #182265) dissolved in anisole (4% by volume) was spin-coated on the copper foil to transfer graphene layers. The Cu foil was etched away using 0.1 M ammonium persulfate ($(NH_4)_2S_2O_8$) for 12 h followed by rinsing in deionized water for 15 min, and then transferred onto 300 nm SiO_2/p^{++} Si wafers for device fabrication. Next, the graphene was patterned using photolithography and O_2 plasma followed by metal contact pattering with Ti/Au (5/50 nm) using thermal evaporation. The width and length of each channel was 10 μm. *I–V* characteristics were measured using Keithley 236 source measurement units. Raman spectra were obtained using a micro-Raman system (Jobin-Yvon, LabRaman HR) with a laser wavelength of 532 nm; intensities were normalized using the G peak.

Fig. 1 shows a schematic illustration of the proton irradiation experiment setup and graphene sample structure. The high energy protons were accelerated to 20 MeV using the MC-50 cyclotron at KIRAMS (Korea Institute of Radiological and Medical Sciences). The obtained protons were then decelerated to the targeted energies of 5, 10, and 15 MeV by changing the number and thickness of aluminum degraders. Each sample was placed in a vacuum chamber with a perpendicular direction to the incident proton beam, and irradiated until the total flux reached 2×10^{14} p/cm^2. Raman spectrum and *I–V* characteristics before and after irradiation were compared to measure the effect of irradiated proton energy. For safety purposes, all measurements were conducted 5 days after irradiation to remove residual radiation.

Fig. 2(a) shows the Raman spectrum of graphene before and after proton irradiation. The pristine graphene before proton irradiation exhibited sharp main peaks positioned at 1583 cm^{-1} and 2680 cm^{-1}. The peak at 1583 cm^{-1} is referred to as the G-peak and originates from the stretching motion of the carbon atoms with an E_{2g} symmetry at **Γ**. The peak at 2680 cm^{-1} is referred to as the 2D peak (or G′ peak), which is due to a double resonance process and is the second order of zone-boundary phonons [14]. The negligible D peak (1341 cm^{-1}) and high intensity of the 2D peak compared to the G-peak confirmed that the graphene was a high quality monolayer.

After proton irradiation of 5, 10, and 15 MeV, the samples exhibited different changes in the Raman spectrum. The most common method for the detection of defect formation in graphene is the observation of a D peak, which is due to the breathing modes of A_{1g} symmetry involving the transverse optical phonons near the Brillouin zone corner **K** [15,16]. Unlike the G and 2D peaks, the D peak requires defects to break the A_{1g} symmetry to achieve double resonance for its activation [15,16]. We found that the D peak, as well as the D + G peak (2934 cm^{-1}), increased after 5 and 10 MeV

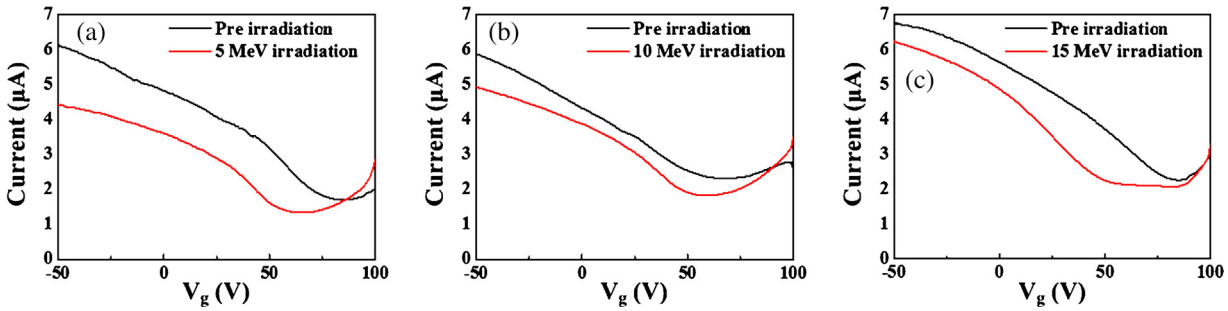

Fig. 3. *I–V* characteristics of graphene transistors before and after (a) 5, (b) 10, and (c) 15 MeV proton irradiation.

proton irradiations while no significant change in the D peak was observed for the 15 MeV irradiated sample. Another defect activated mode known as the Dτ peak (1620 cm^{-1}) was also observed. The Dτ mode is similar to the D mode, but is due to a double resonance as an intra-valley process [16]. Similar to our observations regarding the D peak, formation of the Dτ peak was observed only for the 5 and 10 MeV proton irradiated samples. On the contrary, the D″ peak (1130 cm^{-1}) was observed for all of the graphene samples after proton irradiation. Previous reports have observed a D″ peak in defective and nano diamonds due to sufficient disorder or size to relax the wave vector selection rule [17]. Together, these results indicated that proton irradiation of graphene can induce partial sp^3 type defects. It should be noted that the low intensity of the D″ peak should not be directly compared with other peaks, because the sp^2 sites are 50–230 times more sensitive than the sp^3 sites when using visible light Raman spectroscopy due to insufficient photon energy for σ state excitations [12,15]. In addition, the decrease in the 2D peak intensity in all of the samples shows the damaging effect of proton irradiation.

Fig. 2(b) shows the evolution of the peak intensities as a function of irradiated proton energy. The D, D′ and D + G peak intensities increased when graphene was irradiated with 5 and 10 MeV protons while the D″ peak was observed at every sample which was irradiated with protons. The inequality of the peak characteristics were attributed to the different type of defects generated by irradiation. Due to the 2 dimensional structure of graphene, only a limited number of defects are possible [9], among which the types of defects that can be formed by proton irradiation are primarily vacancy and interstitial defects [11]. However, our results show that a partial sp^3 type defect was also formed after irradiation. Recent reports show that the correlation between D and D′ can be used to classify the formation of vacancy type defects [18]. The obtained value of $I_D/I_{D'}$ = 8–9 for the 5 and 10 MeV samples showed that the majority of the defects were vacancy type defects, indicating that the transferred energy from the protons was sufficient to form vacancies in the graphene lattice. The formation of D, D′, and D + G peaks was consistent with the results of proton irradiated graphene [11,12]. On the contrary, the negligible D, D′ and D + G peaks and the presence of D″ peak for the 15 MeV proton irradiated sample suggested that the generated defects are mostly sp^3 type.

Further electrical characterization was conducted by measuring the electrical characteristics of the graphene field effect transistors. Fig. 3 shows the transfer curve of the graphene transistors before and after irradiation with (a) 5, (b) 10 and (c) 15 MeV protons. After proton irradiation, the Dirac point shifted for the case of 5 and 10 MeV protons, which may have been due to charge buildup in the SiO_2 [19]. The higher degree of shifting by the 5 MeV proton irradiated sample was mainly caused by the higher amount of damage introduced into the SiO_2 layer at the lower proton energy [20]. The current value at the Dirac point also decreased, approximately 21% for both 5 and 10 MeV proton irradiated samples, which was mainly due to the defective nature of graphene. Surprisingly, the 15 MeV proton irradiated sample exhibited a different change in *I–V* characteristics as well as a decrease in current and shift in the Dirac point which resulted in a flat region in the Dirac point. The altered *I–V* characteristic was due to a change in energy band characteristics, and is only found in the 15 MeV proton irradiated graphene. These results were quite different from the change in electrical characteristics of other materials after proton irradiation, which indicated that the smaller amount of damage at higher energies was due to a lower amount of defects [6]. Therefore, 15 MeV protons introduced different types of defects. The exact origin of this change is not fully understood, but in comparison with the Raman spectroscopy results, we suspect that the change was related to sp^3 type defects which can alter the electrical characteristics of graphene from semimetal to even insulating properties [21].

The relationship between the ambiguous results and proton energies can be explained by the different amount of energy transferred during the collision process. Stopping power, which is the conservative force applied to a particle during an interaction, was calculated and simulated on graphite to estimate the effect of proton irradiation. Fig. 4(a) shows the stopping power of protons irradiated onto graphite as a function of proton energy, which was plotted using the Bethe formula with corrections obtained from the National Institute of Standards and Technologies (NIST) PSTAR database [22]. The calculated stopping power of the 5, 10, and 15 MeV protons were 1.20, 0.72, and 0.50 eV/Å, respectively, indicating that protons with lower energies transfer more energy to the target in the MeV range. A Monte Carlo simulation method has also been used to estimate the different effects of proton energy by using stopping and range of ions in matter (SRIM) calculations [23]. Fig. 4(b) shows the stopping power versus depth for 5–15 MeV protons irradiated onto graphite. The simulated penetration depth of protons was ~178, ~605 and ~1237 μm, respectively. Incident protons can generate defects inside or outside a selected layer of graphene. Owing to the large penetration depth compared to the thickness of graphene, the probability of defect formation in a single layer graphene is small [4]. The defect formation in graphene is related to the stopping power at the surface which coincides with the Bethe formula results.

Due to the difference in energy transferred from highly energetic protons, lower energy protons transferred more energy to the graphene lattice. Therefore, it is more likely for 5 MeV proton irradiated graphene to have more defects than samples irradiated with other proton energies, and which resulted in higher D peak formation compared to the 10 MeV proton irradiation. The difference in the transferred energy can also cause different types of defects as demonstrated in our experimental results. The formation of vacancy defects in graphene requires a kinetic barrier T_d of 18–22 eV [9]. Recent time-dependent density function theory simulations of proton irradiation on graphene predicts that the transferred energy from 5–15 MeV protons should be roughly 15–20 eV [24], which is at the boundary of the displacement threshold of T_d. Further, our experimental results showed that the

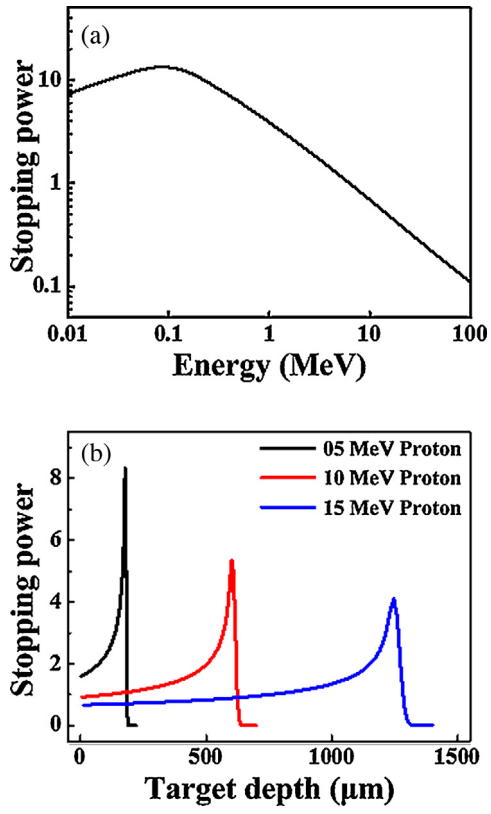

Fig. 4. Energy loss per distance of highly energetic protons traversing graphite (a) verses proton energy plotted by Bethe formula and corrections and (b) verses target depth of 5, 10, and 15 MeV protons by SRIM simulation. The unit of stopping power is eV/Å.

threshold proton energy for vacancy type defects is between 10 and 15 MeV.

In conclusion, we have demonstrated the effect of irradiated proton energy on graphene. Irradiation with 5 and 10 MeV protons resulted in an increase in D and D′ peaks, with peak ratios corresponding to vacancy defects. Irradiation with 15 MeV protons did not result in formation of significant D and D′ peaks; however, a D″ peak did form due to sp^3 type defects. Transistors exhibited a decrease in the current along with Dirac point shifts, but only the 15 MeV proton irradiated sample exhibited flattening at the Dirac point. Theoretical and simulation results indicated that the differences in effects at different proton energies were due to different energy transfer amounts.

Acknowledgements

This work was supported by the Korea Aerospace Research Institute (KARI)-University partnership program and by the Priority Research Centers Program through the National Research Foundation of Korea (NRF) funded by the Ministry of Education, Science and Technology (2012-0006689). This research was also supported in part by the National Research Foundation of Korea (NRF) grant funded by the Korean government (MEST) (No. 2011-0028594) and by the IT R&D program of MOTIE/KEIT [10040052, Development of X-ray Detector Sensor and ROIC on Photon Counting Method for 16bit High Resolution Dynamic Image Processing]. This work was also supported by the Industrial Strategic Technology Development program (10041041, Development of Non-vacuum and Non-lithography Based 5 μm Width Cu Interconnect Technology for TFT Backplane) funded by the Ministry of Knowledge Economy (MKE, Korea).

References

[1] A. Holmes-Siedle, L. Adams, Handbook of Radiation Effects, Oxford University Press, New York, 1993.
[2] M. Ackermann, M. Ajello, A. Allafort, L. Baldini, J. Ballet, G. Barbiellini, M.G. Baring, D. Bastieri, K. Bechtol, R. Bellazzini, R.D. Blandford, E.D. Bloom, E. Bonamente, A.W. Borgland, E. Bottacini, T.J. Brandt, J. Bregeon, M. Brigida, P. Bruel, R. Buehler, G. Busetto, S. Buson, G.A. Caliandro, R.A. Cameron, P.A. Caraveo, J.M. Casandjian, C. Cecchi, Ö. Çelik, E. Charles, S. Chaty, R.C.G. Chaves, A. Chekhtman, C.C. Cheung, J. Chiang, G. Chiaro, A.N. Cillis, S. Ciprini, R. Claus, J. Cohen-Tanugi, L.R. Cominsky, J. Conrad, S. Corbel, S. Cutini, F. D'Ammando, A. de Angelis, F. de Palma, C.D. Dermer, E. do Couto e Silva, P.S. Drell, A. Drlica-Wagner, L. Falletti, C. Favuzzi, E.C. Ferrara, A. Franckowiak, Y. Fukazawa, S. Funk, P. Fusco, F. Gargano, S. Germani, N. Giglietto, P. Giommi, F. Giordano, M. Giroletti, T. Glanzman, G. Godfrey, I.A. Grenier, M.-H. Grondin, J.E. Grove, S. Guiriec, D. Hadasch, Y. Hanabata, A.K. Harding, M. Hayashida, K. Hayashi, E. Hays, J.W. Hewitt, A.B. Hill, R.E. Hughes, M.S. Jackson, T. Jogler, G. Jóhannesson, A.S. Johnson, T. Kamae, J. Kataoka, J. Katsuta, J. Knödlseder, M. Kuss, J. Lande, S. Larsson, L. Latronico, M. Lemoine-Goumard, F. Longo, F. Loparco, M.N. Lovellette, P. Lubrano, G.M. Madejski, F. Massaro, M. Mayer, M.N. Mazziotta, J.E. McEnery, J. Mehault, P.F. Michelson, R.P. Mignani, W. Mitthumsiri, T. Mizuno, A.A. Moiseev, M.E. Monzani, A. Morselli, I.V. Moskalenko, S. Murgia, T. Nakamori, R. Nemmen, E. Nuss, M. Ohno, T. Ohsugi, N. Omodei, M. Orienti, E. Orlando, J.F. Ormes, D. Paneque, J.S. Perkins, M. Pesce-Rollins, F. Piron, G. Pivato, S. Rainò, R. Rando, M. Razzano, S. Razzaque, A. Reimer, O. Reimer, S. Ritz, C. Romoli, M. Sánchez-Conde, A. Schulz, C. Sgrò, P.E. Simeon, E.J. Siskind, D.A. Smith, G. Spandre, P. Spinelli, F.W. Stecker, A.W. Strong, D.J. Suson, H. Tajima, H. Takahashi, T. Takahashi, T. Tanaka, J.G. Thayer, J.B. Thayer, D.J. Thompson, S.E. Thorsett, L. Tibaldo, O. Tibolla, M. Tinivella, E. Troja, Y. Uchiyama, T.L. Usher, J. Vandenbroucke, V. Vasileiou, G. Vianello, V. Vitale, A.P. Waite, M. Werner, B.L. Winer, K.S. Wood, M. Wood, R. Yamazaki, Z. Yang, S. Zimmer, Detection of the characteristic pion-decay signature in supernova remnants, Science 339 (2013) 807–811.
[3] S.M. Khanna, J. Webb, H. Tang, A.J. Houdayer, C. Carlone, 2 MeV proton radiation damage studies of gallium nitride films through low temperature photoluminescence spectroscopy measurements, IEEE Trans. Nucl. Sci. 47 (2000) 2322–2328.
[4] H. Xinwen, A.P. Karmarkar, B. Jun, D.M. Fleetwood, R.D. Schrimpf, R.D. Geil, R.A. Weller, B.D. White, M. Bataiev, L.J. Brillson, U.K. Mishra, Proton-irradiation effects on AlGaN/AlN/GaN high electron mobility transistors, IEEE Trans. Nucl. Sci. 50 (2003) 1791–1796.
[5] H. Xinwen, B.K. Choi, H.J. Barnaby, D.M. Fleetwood, R.D. Schrimpf, L. Sungchul, S. Shojah-Ardalan, R. Wilkins, U.K. Mishra, R.W. Dettmer, The energy dependence of proton-induced degradation in AlGaN/GaN high electron mobility transistors, IEEE Trans. Nucl. Sci. 51 (2004) 293–297.
[6] H.Y. Kim, C.F. Lo, L. Liu, F. Ren, J. Kim, S.J. Pearton, Proton-irradiated InAlN/GaN high electron mobility transistors at 5, 10, and 15 MeV energies, Appl. Phys. Lett. 100 (2012), 012107–012103.
[7] Y. Liu, P.P. Ruden, J. Xie, H. Morkoç, K.-A. Son, Effect of hydrostatic pressure on the dc characteristics of AlGaN/GaN heterojunction field effect transistors, Appl. Phys. Lett. 88 (2006) 013505.
[8] C. Lee, X. Wei, J.W. Kysar, J. Hone, Measurement of the elastic properties and intrinsic strength of monolayer graphene, Science 321 (2008) 385–388.
[9] F. Banhart, J. Kotakoski, A.V. Krasheninnikov, Structural defects in graphene, ACS Nano 5 (2011) 26–41.
[10] G. Ko, H.Y. Kim, F. Ren, S.J. Pearton, J. Kim, Electrical characterization of 5 MeV proton-irradiated few layer graphene, Electrochem. Solid State Lett. 13 (2010) K32–K34.
[11] S. Mathew, T.K. Chan, D. Zhan, K. Gopinadhan, A.R. Barman, M.B.H. Breese, S. Dhar, Z.X. Shen, T. Venkatesan, J.T.L. Thong, The effect of layer number and substrate on the stability of graphene under MeV proton beam irradiation, Carbon 49 (2011) 1720–1726.
[12] S. Mathew, T.K. Chan, D. Zhan, K. Gopinadhan, A. Roy Barman, M.B.H. Breese, S. Dhar, Z.X. Shen, T. Venkatesan, J.T.L. Thong, Mega-electron-volt proton irradiation on supported and suspended graphene: a Raman spectroscopic layer dependent study, J. Appl. Phys. 110 (2011) 084309.
[13] X. Li, W. Cai, J. An, S. Kim, J. Nah, D. Yang, R. Piner, A. Velamakanni, I. Jung, E. Tutuc, S.K. Banerjee, L. Colombo, R.S. Ruoff, Large-area synthesis of high-quality and uniform graphene films on copper foils, Science 324 (2009) 1312–1314.
[14] A.C. Ferrari, J.C. Meyer, V. Scardaci, C. Casiraghi, M. Lazzeri, F. Mauri, S. Piscanec, D. Jiang, K.S. Novoselov, S. Roth, A.K. Geim, Raman spectrum of graphene and graphene layers, Phys. Rev. Lett. 97 (2006) 187401.
[15] A.C. Ferrari, J. Robertson, Interpretation of Raman spectra of disordered and amorphous carbon, Phys. Rev. B 61 (2000) 14095–14107.
[16] A.C. Ferrari, D.M. Basko, Raman spectroscopy as a versatile tool for studying the properties of graphene, Nat. Nanotechnol. 8 (2013) 235–246.
[17] W.A. Yarbrough, A.R. Badzian, D. Pickrell, Y. Liou, A. Inspektor, Diamond deposition at low substrate temperatures, J. Cryst. Growth 99 (1990) 1177–1182.
[18] A. Eckmann, A. Felten, A. Mishchenko, L. Britnell, R. Krupke, K.S. Novoselov, C. Casiraghi, Probing the nature of defects in graphene by Raman spectroscopy, Nano Lett. 12 (2012) 3925–3930.
[19] J.R. Schwank, M.R. Shaneyfelt, D.M. Fleetwood, J.A. Felix, P.E. Dodd, P. Paillet, V. Ferlet-Cavrois, Radiation effects in MOS oxides, IEEE Trans. Nucl. Sci. 55 (2008) 1833–1853.
[20] J.R. Janesick, G.B. Soli, T.S. Elliott, S.A. Collins, Effects of proton damage on charge-coupled devices, in: Proc. SPIE – Int. Soc. Opt. Eng., 1991, pp. 87–108.

[21] D.C. Elias, R.R. Nair, T.M.G. Mohiuddin, S.V. Morozov, P. Blake, M.P. Halsall, A.C. Ferrari, D.W. Boukhvalov, M.I. Katsnelson, A.K. Geim, K.S. Novoselov, Control of graphene's properties by reversible hydrogenation: evidence for graphane, Science 323 (2009) 610–613.
[22] M.J. Berger, J. Coursey, M. Zucker, J. Chang, Stopping-power and Range Tables for Electrons, Protons, and Helium Ions, NIST Physics Laboratory, 1998.
[23] J.F. Ziegler, M.D. Ziegler, J.P. Biersack, SRIM – the stopping and range of ions in matter (2010), Nucl. Instrum. Methods Phys. Res. Sec. B: Beam Interact. Mater. Atoms 268 (2010) 1818–1823.
[24] S. Bubin, B. Wang, S. Pantelides, K. Varga, Simulation of high-energy ion collisions with graphene fragments, Phys. Rev. B 85 (2012) 235435.